JOC Article

Nile Red Nucleoside: Design of a Solvatofluorochromic Nucleoside as an Indicator of Micropolarity around DNA

Akimitsu Okamoto,* Kazuki Tainaka, and Yoshimasa Fujiwara

Department of Synthetic Chemistry and Biological Chemistry, Faculty of Engineering, Kyoto University, Kyoto 615-8510, Japan

okamoto@sbchem.kyoto-u.ac.jp

Received January 25, 2006

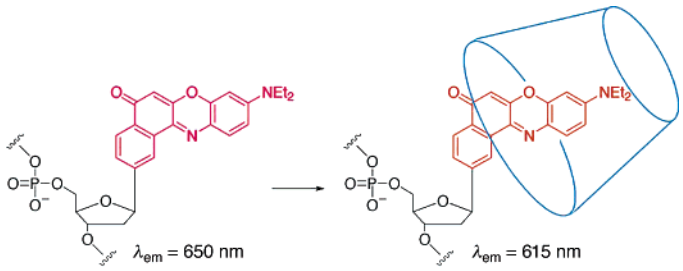

The fluorophore, Nile Red, effectively works as a polarity-sensitive fluorescence probe. We have designed a new nucleoside modified by Nile Red for examining the change in the polarity of the microenvironment surrounding DNA. We synthesized a Nile Red nucleoside (**1**), formed by replacing nucleobases with Nile Red, through the coupling of a 2-hydroxylated Nile Red derivative and 1,2-dideoxyglycan. This nucleoside showed a high solvatofluorochromicity. The fluorescence of **1** incorporated into DNA was greatly shifted to shorter wavelength by the addition of β-cyclodextrin. The photophysical function of the Nile Red nucleoside will be a good optical indicator for monitoring the change in the micropolarity properties at a specific site on target sequences with interaction between DNA and DNA-binding molecules.

Introduction

Local variations in the structure and dynamics of biomolecules play important roles in mediating the interaction events between biomolecules. Monitoring of the microenvironmental change in DNA and its surroundings is extremely important because the structure of DNA itself and the formation of DNA−protein complexes are strongly influenced by their microenvironmental conditions. For such a purpose, fluorescent probes that can be site-specifically incorporated into the DNA sequence of interest and are sensitive to the change in its microenvironment are highly valuable and desirable.[1] Nucleosides possessing various fluorophores have been explored for studying the structures and dynamics of nucleic acids, including fluorescent nucleoside analogues, as exemplified by 2-aminopurine,[2] ethynyl-extended nucleobase derivatives,[3] and nucleoside analogues replaced by flat aromatic fluorophores.[4]

Solvatochromic fluorophores, which show shifts in absorption and emission bands induced by a change in solvent nature or composition, are useful for monitoring the structural transformation and intermolecular interaction of biomolecules with micropolarity change in the surroundings.[5] The well-known fluorophore, Nile Red, is a hydrophobic, highly fluorescent,

* To whom correspondence should be addressed. Phone: +81-75-383-2755. FAX: +81-75-383-2759.

(1) (a) Wojczewski, C.; Stolze, K.; Engels, J. W. *Synlett* **1999**, 1667−1678. (b) Hawkins, M. E. *Cell Biochem. Biophys.* **2001**, *34*, 257−281. (c) Okamoto, A.; Saito, Y.; Saito, I. *J. Photochem. Photobiol. C* **2005**, *6*, 108−122.

(2) (a) Ward, D. C.; Reich, E.; Stryer, L. *J. Biol. Chem.* **1969**, *244*, 1228−1237. (b) Menger, M.; Tuschl, T.; Eckstein, F.; Porschke, D. *Biochemistry* **1996**, *35*, 14710−14716. (c) Lacourciere, K. A.; Stivers, J. T.; Marino, J. P. *Biochemistry* **2000**, *39*, 5630−5641.

(3) (a) Seela, F.; Zulauf, M.; Sauer, M.; Deimel, M. *Helv. Chim. Acta* **2000**, *83*, 910−927. (b) Hurley, D. J.; Seaman, S. E.; Mazura, J. C.; Tor, Y. *Org. Lett.* **2002**, *4*, 2305−2308. (c) Okamoto, A.; Kanatani, K.; Saito, I. *J. Am. Chem. Soc.* **2004**, *126*, 4820−4827. (d) Okamoto, A.; Tainaka, K.; Saito, I. *Bioconjugate Chem.* **2005**, *16*, 1105−1111. (e) Okamoto, A.; Tainaka, K.; Nishiza, K.-i.; Saito, I. *J. Am. Chem. Soc.* **2005**, *127*, 13128−13129.

(4) (a) Strässler, C.; Davis, N. E.; Kool, E. T. *Helv. Chim. Acta* **1999**, *82*, 2160−2171. (b) Kool, E. T. *Acc. Chem. Res.* **2002**, *35*, 936−943. (c) Okamoto, A.; Tainaka, K.; Saito, I. *J. Am. Chem. Soc.* **2003**, *125*, 4972−4973. (d) Okamoto, A.; Tainaka, K.; Saito, I. *Tetrahedron Lett.* **2003**, *44*, 6871−6874.

(5) (a) Okamoto, A.; Tanaka, K.; Fukuta, T.; Saito, I. *J. Am. Chem. Soc.* **2003**, *125*, 9296−9297. (b) Jadhav, V. R.; Barawkar, D. A.; Ganesh, K. N. *J. Phys. Chem. B* **1999**, *103*, 7383−7385. (c) Kimura, K.; Kawai, K.; Majima, T. *Org. Lett.* **2005**, *7*, 5829−5832.

10.1021/jo060168o CCC: $33.50
Published on Web 04/04/2006

SCHEME 1. Synthesis of Nile Red Nucleoside (1) and 1-Containing ODN

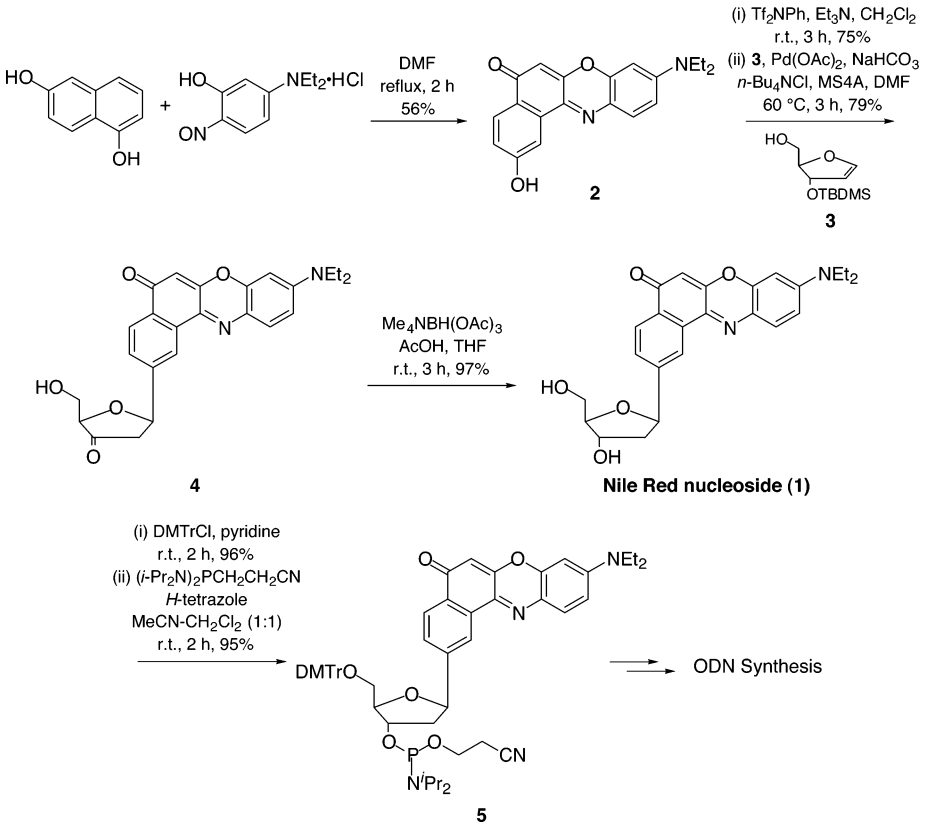

solvatochromic dye that has been extensively applied to examine the local polarity in zeolites[6] and micelles[7] and is among the most promising candidates for a microenvironment-sensitive fluorescent probe.[8] Thus, Nile Red derivatives incorporated into DNA would also be useful as polarity-sensitive fluorescence probes for examining the change in polarity of the microenvironments around DNA. In particular, when Nile Red is fixed in the place of a nucleobase to oligodeoxynucleotide (ODN) probes, the change in the micropolarity properties around a specific site on the target sequences would be easily monitored.

We herein report the sequence-selective fluorescence labeling of DNA with Nile Red and the solvatochromic function of Nile Red fixed to DNA as a fluorescent reporter for micropolarity. We synthesized a Nile Red nucleoside (**1**), produced by the replacement of a nucleobase by Nile Red. This nucleoside showed a high solvatofluorochromicity, just like free Nile Red, and the fluorescence of **1** incorporated to DNA also greatly varied with micropolarity to function as an effective micropolarity indicator.

Results and Discussion

The outline of the synthesis of a Nile Red nucleoside is shown in Scheme 1. We prepared a 2-hydroxylated Nile Red derivative **2** from 1,6-dihydroxynaphthalene and 5-diethylamino-2-nitroso-1-phenol according to a protocol reported previously (56%).[9] Compound **2** was converted into a triflate derivative (75%). Subsequently, we obtained compound **4** β-selectively (79%) through Heck reaction between **2** and 1,2-dideoxyglycan **3** given by depyrimidination of thymidine by means of fragmentation at elevated temperatures in the presence of hexamethyldisilazane.[10] A carbonyl group at 3′-C of **4** was then stereoselectively reduced with tetramethylammonium triacetoxyborohydride to give Nile Red nucleoside (**1**) (97%).

We initially examined the photochemical properties of **1** in nine different solvents. Both absorption maximum and fluorescence emission wavelength shifted to longer wavelength as the polarity parameter E_T of the solvents[11] increased (Figure 1 and Table 1). The absorption maximum greatly changed with solvent polarity, for example, from 506 nm in diethyl ether to 524 nm in ethyl acetate, 537 nm in acetonitrile, and 573 nm in formamide (Figure 1a). The shift of the absorption maximum to longer wavelength with higher polarity indicates that **1** retains the solvatochromic property observed for Nile Red. The fluorescence emission peak was observed at 561 nm in diethyl ether, 584 nm in ethyl acetate, 606 nm in acetonitrile, and 637 nm in formamide (Figure 1b). The fluorescence emission peaks were also red-shifted with higher solvent polarity, suggesting that **1** works as a highly solvatofluorochromic nucleoside. As

(6) (a) Uppili, S.; Thomas, K. J.; Crompton, E. M.; Ramamurthy, V. *Langmuir* **2000**, *16*, 265−274. (b) Meinershagen, J. L.; Bein, T. *J. Am. Chem. Soc.* **1999**, *121*, 448−449.

(7) (a) Datta, A.; Mandal, D.; Pal, S. K.; Bhattacharyya, K. *J. Phys. Chem. B* **1997**, *101*, 10221−10225. (b) Maiti, N. C.; Krishna, M. M. G.; Britto, P. J.; Periasamy, N. *J. Phys. Chem. B* **1997**, *101*, 11051−11060.

(8) (a) Goloni, C. M.; Williams, B. W.; Foresman, J. B. *J. Fluorescence* **1998**, *8*, 395−404. (b) Deye, J. F.; Berger, T. A.; Anderson, A. G. *Anal. Chem.* **1990**, *62*, 615−622.

(9) (a) Nagy, K.; Göktürk, S.; Biczók, L. *J. Phys. Chem. A* **2003**, *107*, 8784−8790. (b) Briggs, M. S. J.; Bruce, I.; Miller, J. N.; Moody, C. J.; Simmonds, A. C.; Swann, E. *J. Chem. Soc., Perkin Trans. 1* **1997**, 1051−1058.

(10) Coleman. R. S.; Madaras, M. L. *J. Org. Chem.* **1998**, *63*, 5700−5703.

(11) Mulov, S. L.; Carmichael, I.; Hug, G. L. *Handbook of Photochemistry*; Marcel Dekker: New York, 1993.

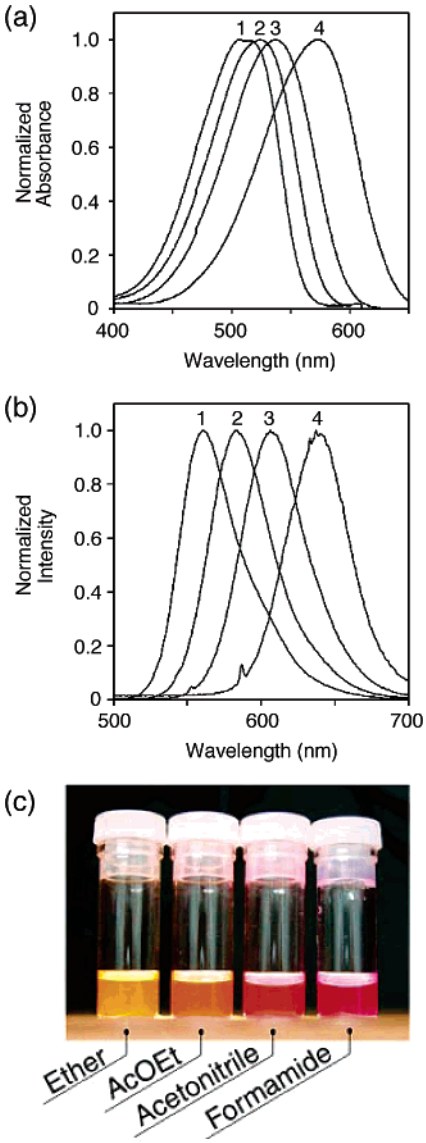

FIGURE 1. Absorption and fluorescence of **1**. Spectra were measured using 10 μM **1** in different solvents at 20 °C. (a) Absorption spectra of **1** in different solvents. Peak 1, in diethyl ether; peak 2, in ethyl acetate; peak 3, in acetonitrile; peak 4, in formamide. (b) Fluorescence emission spectra of **1** in different solvents. Peak 1, in diethyl ether; peak 2, in ethyl acetate; peak 3, in acetonitrile; peak 4, in formamide. (c) Fluorescence colors of **1** in different solvents. The sample solutions were illuminated through a 450 nm long pass filter.

shown in Figure 1c, the fluorescence color of **1** vividly changed according to the polarity of solvents.

Nucleoside **1** was incorporated efficiently into an ODN according to a conventional phosphoramidite method after protection of **1** (96%) and conversion into the phosphoramidite form (95%). Using the ODN 5′-d(GCGTTA**1**ATTGCG)-3′, we examined the melting temperatures (T_m) and thermodynamic parameters of six different duplexes with the complement 5′-d(CGCAATT**N**TAACGC)-3′ (**N** = A, G, C, T, and abasic nucleotide (1′,2′-dideoxyribose, Ap)) or 5′-d(CGCAATTAACGC)-3′ in a buffer solution of 50 mM sodium phosphate (pH = 7.0) and 100 mM sodium chloride. The results were unequivocally separable into two types of duplexes (Table 2). Group I consists of duplexes possessing C, T, or Ap as a base opposite **1**. T_m was relatively high (50−54 °C), and ΔH and ΔS were −74 to −78 kcal mol^{-1} and −200 to −211 cal mol^{-1} K^{-1}, respectively. Group II, which consists of duplexes possessing A or G as a base opposite **1** and a duplex possessing a single-base bulge of **1** ("no base" in Table 2), has T_m values ca. 5 °C lower than that of Group I (45−48 °C). The ΔH and ΔS calculated were −52 to −60 kcal mol^{-1} and −135 to −156 cal mol^{-1} K^{-1}, respectively. The values of T_m and ΔH suggest that the Nile Red fluorophore of Group I would bind to the duplex tightly and contribute to duplex stabilization, as compared with the fluorophore of Group II.

TABLE 1. Absorption and Fluorescence Properties of 1 in Different Solvents[a]

solvents	E_T[b]	λ_{ab} (nm)	ϵ_{max} ($\times 10^3$)	λ_{em} (nm)	Φ
diethyl ether	34.6	506	4.12	561	0.35
dioxane	36.0	522	3.56	572	0.31
ethyl acetate	38.1	524	3.93	584	0.30
chloroform	39.1	546	4.47	596	0.22
N,*N*-dimethylformamide	43.8	545	3.79	613	0.28
dimethyl sulfoxide	45.0	555	3.63	618	0.19
acetonitrile	46.0	537	4.16	606	0.20
methanol	55.5	557	3.38	632	0.09
formamide	56.6	573	3.32	637	0.10

[a] Condition: 10 μM **1** in different solvents at 20 °C. [b] Reported in ref 10.

TABLE 2. Melting Temperatures (T_m) of Duplexes Containing Nile Red

N	T_m (°C)[a]	$-\Delta H$ (kcal mol^{-1})[b]	$-\Delta S$ (cal mol^{-1} K^{-1})[b]	$-\Delta G_{298}$[b]
A	44.8	52.3	135	12.1
G	47.6	59.5	156	13.1
C	50.4	75.6	207	13.8
T	50.8	73.9	200	14.8
Ap	54.4	77.9	211	15.0
no base	45.5	55.7	147	11.8

[a] 2.5 μM 5′-d(GCGTTA**1**ATTGCG)-3′/5′-d(CGCAATNTAACGC)-3′ in 50 mM sodium phosphate (pH = 7.0) and 0.1 M sodium chloride. [b] Thermodynamic parameters were calculated from T_m values of 10, 5, 2.5, and 1.25 μM duplex in 50 mM sodium phosphate (pH = 7.0) and 0.1 M sodium chloride.

These duplexes showed only a small difference in their photophysical properties (Figure 2a). The absorption maxima of single-stranded and double-helical ODNs, except for a bulge duplex, were observed at 607−609 nm. The absorption maximum of a bulge duplex was observed at 603 nm, but it is a very slight shift. The fluorescence emission peak of **1**-containing ODN was also almost constant at ∼650 nm regardless of the type of hybridized strands (Figure 2b). The very small shift of absorption maximum and fluorescence emission peak suggests that the micropolarity around **1** in duplexes is not significantly changed by the nature of bases opposite **1** in the duplex.

β-Cyclodextrin has been recognized as one of the most important host materials for organic molecules in aqueous media and as the donor of a hydrophobic microenvironment.[12] This host molecule is known to form an inclusion complex with Nile Red.[13] In this complex, the electron-donating diethylamino group of Nile Red is placed in the nanocavity of β-cyclodextrin, and

(12) (a) Breslow, R. *Acc. Chem. Res.* **1995**, *28*, 146−153. (b) Szejtli, J. *Chem. Rev.* **1998**, *98*, 1743−1753. (c) Connors, K. A. *Chem. Rev.* **1997**, *97*, 1325−1357.

(13) (a) Hazra, P.; Chakrabarty, D.; Chakraborty, A.; Sarkar, N. *Chem. Phys. Lett.* **2004**, *388*, 150−157. (b) Srivatsavoy, V. J. P. *J. Lumin.* **1999**, *82*, 17−23.

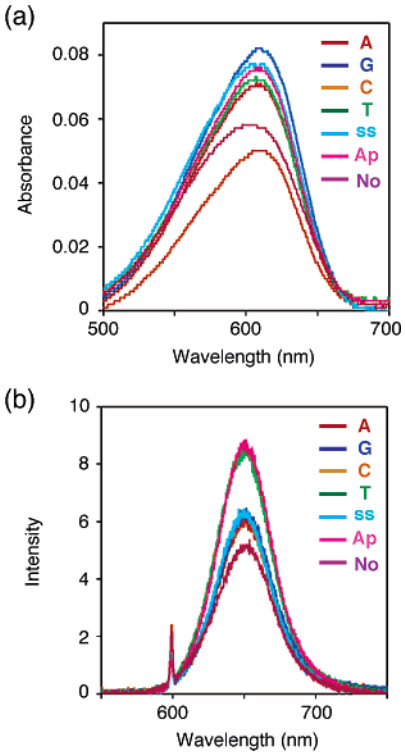

FIGURE 2. Absorption and fluorescence spectra for different structural contexts of **1**-containing ODN. Spectra were measured using a 2.5 μM sample in 50 mM sodium phosphate (pH = 7.0) and 100 mM sodium chloride at 20 °C. A, G, C, and T, 5′-d(GCGTTA**1**ATTGCG)-3′/5′-d(CGCAAT**N**TAACGC)-3′ (**N** = A, G, C, and T, respectively); ss, 5′-d(GCGTTA**1**ATTGCG)-3′; Ap, 5′-d(GCGTTA**1**ATTGCG)-3′/5′-d(CGCAAT**Ap**TAACGC)-3′ (**Ap** = abasic site); No, 5′-d(GCGTTA**1**ATTGCG)-3′/5′-d(CGCAATTAACGC)-3′. (a) Absorption spectra. (b) Fluorescence emission spectra. Excitation wavelength was 600 nm.

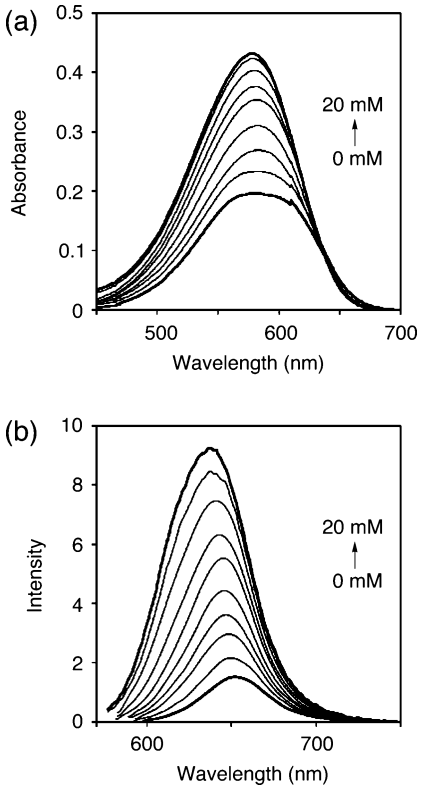

FIGURE 3. Changes in absorption and fluorescence spectra of **1** dependent on β-cyclodextrin concentration. Spectra of 10 μM **1** in water were measured when β-cyclodextrin concentration was 0, 0.125, 0.25, 0.5, 1, 2, 5, 10, 15, and 20 mM. (a) Absorption spectra. (b) Fluorescence emission spectra. Excitation wavelength was 560 nm.

thus β-cyclodextrin would work as an additive for effectively controlling the micropolarity around nucleoside **1**. We measured the photophysical properties of **1** (10 μM) in water with gradually changing concentration of β-cyclodextrin (0 to 20 mM) (Figure 3a). The absorption spectrum was broad and the maximum was observed at 580 nm before the addition of β-cyclodextrin. The absorption spectra became sharper as β-cyclodextrin was added, and the maximum was slightly blue shifted to 578 nm in the presence of 20 mM β-cyclodextrin. Absorbance in 20 mM β-cyclodextrin increased to 2.2 times its original value. An isosbestic point appeared at 638 nm on addition of β-cyclodextrin, suggesting that β-cyclodextrin binds to **1** in a single binding mode. Changes in the fluorescence emission spectra were larger than in the absorption spectra. The fluorescence emission spectra of **1** in water with gradually changing concentration of β-cyclodextrin on excitation at 560 nm are shown in Figure 3b. A fluorescence peak was observed at 651 nm before the addition of β-cyclodextrin. On successive addition of β-cyclodextrin, the spectrum gradually exhibited a hypsochromic shift, and finally at 20 mM β-cyclodextrin the peak maximum was at ~637 nm. The 14-nm blue shift in emission spectra and the increase in fluorescent intensity indicate the formation of an inclusion complex between **1** and β-cyclodextrin. The binding of β-cyclodextrin to **1** results in the exclusion of solvent molecules from the surrounding of Nile Red and a decrease of the micropolarity around **1**. The binding constant K_b was determined as 1.26 M^{-1} at 298 K, from the slope and intercept of a straight line obtained from the plot of $1/(I - I_0)$ versus the reciprocal of the β-cyclodextrin concentration.[14] Additionally, on addition of β-cyclodextrin the fluorescence intensity increased to 6.2 times the original intensity. This is probably due to retardation of the nonradiative rate in the β-cyclodextrin cavity because of the prevention of the rotational freedom of the diethylamino group and the decrease in the polarity inside the cavity.[15]

Having established the blue shift of the fluorescence spectrum of **1** by the formation of a **1**-β-cyclodextrin inclusion complex, we measured the fluorescence emission spectra of the duplexes of **1**-containing ODN, 5′-d(GCGTTA**1**ATTGCG)-3′, and ODNs containing different bases to form a pair with **1**, 5′-d(CGCAAT-**N**TAACGC)-3′, in the presence of 10 mM β-cyclodextrin. When **N** was C, T, or Ap, the fluorescence emission peak was observed at approximately 650 nm, which was only slightly shifted from the fluorescence spectra of duplex samples without β-cyclodextrin shown in Figure 2b (Figure 4a). This result suggests that β-cyclodextrin added to sample solutions does not interact with **1** in these duplexes. On the other hand, when **N** was A, G, or missing, a shoulder at the shorter wavelength side of the spectra appeared (Figure 4b). Particularly, for a bulge duplex, the fluorescence emission maximum shifted to 620 nm. The peak shift to a shorter wavelength suggests that a complex of the **1**-containing ODN and β-cyclodextrin was formed. The

(14) de la Pena, A. M.; Ndou, T.; Zung, J. B.; Warner, I. M. *J. Phys. Chem.* **1991**, *95*, 3330−3334.
(15) (a) Krishna, M. M. G. *J. Phys. Chem. A* **1999**, *103*, 3589−3595. (b) Sarkar, N.; Das, K.; Nath, D. N.; Bhattacharyya, K. *Langmuir* **1994**, *10*, 326−329.

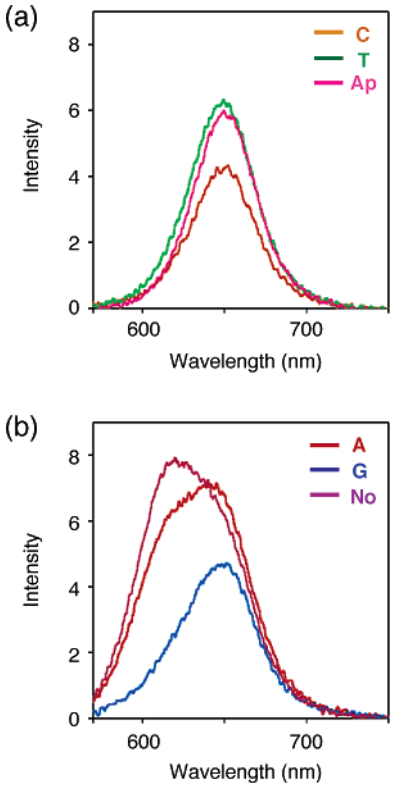

FIGURE 4. Changes in fluorescence spectra of **1**-containing ODN dependent on the nature of the complementary base in the presence of β-cyclodextrin. Spectra were measured using a 2.5 μM sample and 10 mM β-cyclodextrin in 50 mM sodium phosphate (pH = 7.0) and 100 mM sodium chloride at 20 °C. Excitation wavelength was 560 nm. A, G, C, and T, 5′-d(GCGTTA**1**ATTGCG)-3′/5′-d(CGCAAT**N**TAACGC)-3′ (**N** = A, G, C, and T, respectively); ss, 5′-d(GCGTTA**1**ATTGCG)-3′; Ap, 5′-d(GCGTTA**1**ATTGCG)-3′/5′-d(CGCAAT**Ap**TAACGC)-3′ (**Ap** = abasic site); No, 5′-d(GCGTTA**1**ATTGCG)-3′/5′-d(CGCAATTAACGC)-3′. (a) Small peak shift observed for a duplex where the base opposite **1** was C, T, or abasic nucleotide. (b) Large peak shift observed for a duplex where the base opposite **1** was A, G, or missing.

classification of duplexes based on the changes in fluorescence spectra by the addition of β-cyclodextrin was in good agreement with the two groups classified based on thermodynamic stabilities shown in Table 2.

The fluorescence spectra of Group II, shown in Figure 4b, were deconvoluted into two overlapping signals. When a 650-nm-centered fluorescence peak was subtracted from the original fluorescence spectrum, a peak whose maximum wavelength was 615 nm appeared (Figure 5). The peak at 615 nm is a new signal that appears as a result of β-cyclodextrin addition to a sample solution. The appearance of a new peak with a shorter wavelength indicates the formation of an inclusion complex between **1** in the duplex and β-cyclodextrin and a significant decrease of the micropolarity around **1** in the duplex. The fluorescence at 615 nm roughly corresponds to the polarity of DMF as shown in Table 1. The **1** of Group II would slide out of a π-stacking array in a double-helical structure because of the existence of the purine base opposite **1** or the formation of a bulge structure. Actually, the T_m of Group II was lower than that for Group I as described above, suggesting that any intercalation of **1** to a double-helical structure was lost or very slight. Therefore, **1** in these structures could easily be

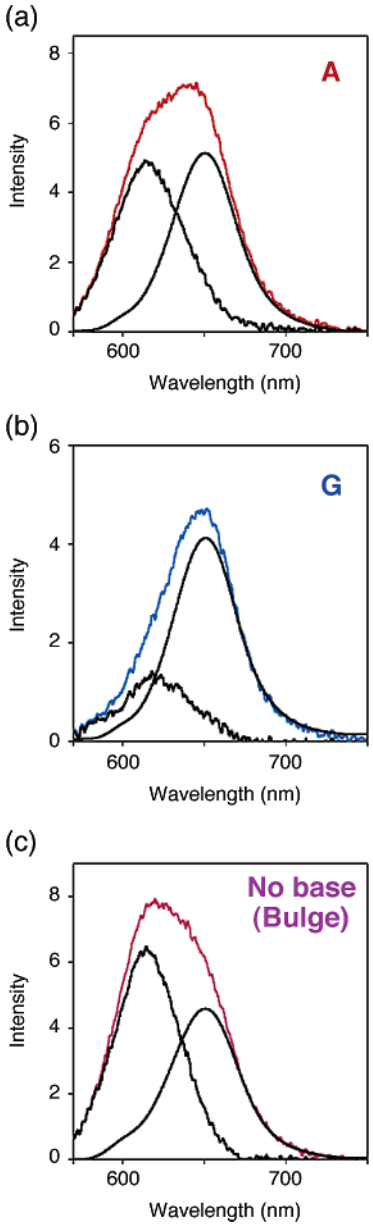

FIGURE 5. Fluorescence spectra deconvoluted into two peaks. Fluorescence spectra of **1**-containing ODN in the presence of β-cyclodextrin in Figure 4 were analyzed. (a) 5′-d(GCGTTA**1**ATTGCG)-3′/5′-d(CGCAAT**A**TAACGC)-3′. (b) 5′-d(GCGTTA**1**ATTGCG)-3′/5′-d(CGCAAT**G**TAACGC)-3′. (c) 5′-d(GCGTTA**1**ATTGCG)-3′/5′-d(CGCAATTAACGC)-3′.

included by β-cyclodextrin possessing an interior space of low polarity, resulting in a fluorescence spectrum with a shorter wavelength.

Conclusion

In conclusion, we have synthesized a polarity-sensitive Nile Red nucleoside and a nucleic acid containing it. These sensitively changed fluorescence wavelength according to the change of micropolarity. The fluorescence of the Nile Red fixed in a DNA duplex was greatly shifted to shorter wavelength by the addition of β-cyclodextrin. The photophysical function of the Nile Red nucleoside will be a good optical indicator for monitoring the change in the micropolarity properties at a

specific site on target sequences with interaction between DNA and other DNA-binding molecules.

Experimental Section

1′-*C*-(2-Nile Red)-2′-deoxy-3′-ketoriboside (4). To a solution of **2** (4.01 g, 12 mmol), which was synthesized according to ref 9 (56% yield), in dichloromethane (300 mL) and triethylamine (50 mL) was added *N*-phenyl bis(trifluoromethanesulfonimide) (4.29 g, 12 mmol) at 0 °C, and the mixture was stirred for 3 h at ambient temperature. After concentration, the crude product was purified by column chromatography on silica gel, eluting with hexanes−ethyl acetate (3:1) to give a triflate (4.2 g, 75%) as a dark purple solid: ^{1}H NMR (400 MHz, $CDCl_3$) δ = 8.54 (d, 1H, J = 2.6), 8.41 (d, 1H, J = 8.6), 7.66 (d, 1H, J = 9.0), 7.50 (dd, 1H, J = 8.6, 2.6), 6.72 (dd, 1H, J = 9.2, 2.7), 6.50 (d, 1H, J = 2.6), 6.41 (s, 1H), 3.50 (quartet, 4H, J = 7.1 Hz), 1.29 (t, 6H, J = 7.1 Hz); ^{13}C NMR (100 MHz, $CDCl_3$) δ = 182.0, 152.7, 151.6, 151.4, 147.1, 134.3, 131.7, 129.5, 128.6, 126.9, 125.3, 123.2, 122.1, 116.3, 105.3, 96.2, 45.3, 12.6; FABMS, *m*/*z* 466 [M$^+$]; HRMS calcd for $C_{21}H_{17}N_2O_5F_3S$ [M$^+$] 466.0810, found 466.0806.

To a solution of a triflate (141 mg, 0.3 mmol) in *N*,*N*-dimethylformamide (3 mL) were added $NaHCO_3$ (76 mg, 0.9 mmol), *n*-tetrabutylammonium chloride (84 mg, 0.3 mmol), 4 Å molecular sieves (141 mg), and palladium(II) acetate (17 mg, 0.075 mmol). A solution of glycal 3 (207 mg, 0.9 mmol), which was prepared according to a protocol previously reported,[9] in *N*,*N*-dimethylformamide (1 mL) was added, and the mixture was stirred for 3 h at 60 °C. The reaction mixture was filtered through Celite (chloroform wash), and then the filtrate was extracted with ethyl acetate and saturated aqueous $NaHCO_3$. After concentration, the crude product was purified by column chromatography on silica gel, eluting with hexanes−ethyl acetate (1:2) to give **4** (103 mg, 79%) as a dark purple solid: ^{1}H NMR (400 MHz, $CDCl_3$) δ = 8.63 (d, 1H, J = 1.3), 8.29 (d, 1H, J = 8.1), 7.70 (dd, 1H, J = 8.1, 1.7), 7.59 (d, 1H, J = 9.2), 6.66 (dd, 1H, J = 9.2, 2.7), 6.46 (d, 1H, J = 2.6), 6.36 (s, 1H), 5.41 (dd, 1H, J = 11.1, 5.8), 4.13 (t, 1H, J = 3.4), 4.06 (dd, 1H, J = 12.2, 3.3), 4.02 (dd, 1H, J = 12.2, 3.6), 3.47 (quartet, 4H, J = 7.1), 3.00 (dd, 1H, J = 17.9, 5.9), 2.65 (dd, 1H, J = 17.9, 11.0), 1.70 (br, 1H), 1.27 (t, 6H, J = 7.1); ^{13}C NMR (100 MHz, $CDCl_3$) δ = 213.2, 183.2, 152.3, 151.0, 146.9, 143.1, 139.4, 132.3, 131.7, 131.2, 127.4, 126.5, 124.9, 121.3, 109.8, 105.8, 96.3, 82.6, 77.5, 61.6, 45.4, 45.1, 12.6; FABMS, *m*/*z* 433 [M + H$^+$]; HRMS calcd for $C_{25}H_{25}N_2O_5$ [M + H$^+$] 433.1763, found 433.1763.

1′-*C*-(2-Nile Red)-2′-deoxyriboside (1). A solution of **4** (48 mg, 0.11 mmol), tetramethylammonium triacetoxyborohydride (162 mg, 0.77 mmol), and acetic acid (20 μL) in 2 mL of tetrahydrofuran was stirred for 3 h at ambient temperature. The resulting mixture was concentrated in vacuo and diluted with ethyl acetate. This solution was washed with saturated aqueous NH_4Cl and brine, dried over $MgSO_4$, filtered, and evaporated. The residue was purified by column chromatography on silica gel, eluting with chloroform−methanol (20:1) to give **1** (47 mg, 97%) as a dark purple solid: ^{1}H NMR (400 MHz, DMSO-d_6) δ = 8.61 (s, 1H), 8.29 (d, 1H, J = 8.2), 7.65−7.62 (m, 2H), 6.69 (d, 1H, J = 9.2), 6.49 (s, 1H), 6.39 (s, 1H), 5.39 (dd, 1H, J = 10.3, 5.9), 4.53−4.52 (m, 1H), 4.13−4.10 (m, 1H), 3.93 (dd, 1H, J = 11.7, 3.9), 3.84 (dd, 1H, J = 11.7, 4.9), 3.48 (quartet, 4H, J = 7.1), 2.41 (ddd, 1H, J = 13.2, 5.7, 1.8), 2.14 (ddd, 1H, J = 13.3, 10.1, 6.3), 1.27 (t, 6H, J = 7.1); ^{13}C NMR (100 MHz, DMSO-d_6) δ = 181.9, 151.9, 150.9, 146.6, 146.4, 138.4, 131.6, 131.0, 130.3, 127.5, 125.3, 124.3, 120.5, 110.3, 104.6, 96.1, 88.2, 79.1, 72.5, 62.5, 44.6, 43.7, 12.6; FABMS, *m*/*z* 434 [M$^+$]; HRMS calcd for $C_{25}H_{26}N_2O_5$ [M$^+$] 434.1842, found 434.1847.

1′-*C*-(2-Nile Red)-3′-*O*-(2-cyanoethyl-*N*,*N*′-diisopropylphosphoramidite)-5′-*O*-(4,4′-dimethoxytrityl)-2′-deoxyriboside (5). To a solution of 1 (300 mg, 0.69 mmol) in pyridine (5 mL) was added 4,4′-dimethoxytrityl chloride (155 mg, 0.83 mmol), and the mixture was stirred for 2 h at ambient temperature. The reaction mixture was concentrated and purified by column chromatography on silica gel, eluting with chloroform−methanol (30:1) to give the 5′-protected nucleoside (492 mg, 96%) as a purple solid: ^{1}H NMR (400 MHz, $CDCl_3$) δ = 8.69 (d, 1H, J = 0.9 Hz), 8.27 (d, 1H, J = 8.1 Hz), 7.68 (dd, 1H, J = 8.2, 1.3 Hz), 7.50 (dd, 2H, J = 8.1, 1.3 Hz), 7.39 (dd, 4H, J = 9.0, 1.6 Hz), 7.34 (d, 1H, J = 9.2 Hz), 7.27 (t, 2H, J = 7.5 Hz), 7.18 (t, 1H, J = 7.7 Hz), 6.81 (d, 4H, J = 9.0 Hz), 6.58 (dd, 1H, J = 9.2, 2.7 Hz), 6.45 (d, 1H, J = 2.7 Hz), 6.36 (s, 1H), 5.39 (dd, 1H, J = 10.1, 5.7 Hz), 4.48−4.46 (m, 1H), 4.14 (dd, 1H, J = 7.3, 4.6 Hz), 3.75 (s, 6H), 3.45 (q, 4H, J = 7.1 Hz), 3.43−3.36 (m, 2H), 2.39 (ddd, 1H, J = 13.2, 5.7, 1.8 Hz), 2.15 (ddd, 1H, J = 13.0, 10.1, 6.0 Hz), 2.00 (br. s, 1H), 1.25 (t, 6H, J = 7.0 Hz); ^{13}C NMR (100 MHz, $CDCl_3$) δ = 183.5, 158.5, 152.2, 150.7, 146.7, 145.7, 144.8, 136.1, 132.2, 131.2, 131.1, 130.1, 128.3, 127.8, 127.5, 126.8, 126.0, 124.9, 121.1, 113.2, 109.6, 105.7, 96.2, 86.6, 86.3, 79.8, 74.6, 64.4, 55.2, 45.0, 44.1, 12.6; FABMS, *m*/*z* 736 [M$^+$]; HRMS calcd for $C_{46}H_{44}N_2O_7$ [M$^+$] 736.3149, found 736.3147.

To a solution of the 5′-protected nucleoside (74 mg, 0.10 mmol) and tetrazole (7.0 mg, 0.10 mmol) in 1:1 acetonitrile−dichloromethane (1.0 mL) was added 2-cyanoethyl tetraisopropylphosphordiamidite (63.4 μL, 0.20 mmol) under nitrogen. The mixture was stirred at ambient temperature for 1 h. The resulting mixture was diluted with ethyl acetate, washed with saturated aqueous $NaHCO_3$ and brine, and dried over $MgSO_4$. After removal of solvent, the residue was purified by column chromatography on silica gel, eluting with hexanes−ethyl acetate (1:1) to give a diastereomeric mixture of **5** (89 mg, 95%) as a dark purple oil: ^{1}H NMR (400 MHz, $CDCl_3$) δ = 8.75 (d, 1H, J = 1.3 Hz), 8.73 (d, 1H, J = 1.1 Hz), 8.29 (d, 1H, J = 8.2 Hz), 8.28 (d, 1H, J = 8.2 Hz), 7.73 (dd × 2, 1H × 2, J = 1.8, 8.2 Hz), 7.54−7.51 (2H × 2), 7.42−7.38 (4H × 2), 7.33−7.24 (4H × 2), 7.15−7.20 (1H × 2), 6.82−6.79 (4H × 2), 6.59−6.55 (1H × 2), 6.46 (s, 1H), 6.45 (s, 1H), 6.38 (s × 2, 1H × 2), 5.40−5.35 (1H × 2), 4.57−4.53 (1H × 2), 4.33−4.28 (1H × 2), 3.91−3.79 (1H × 2), 3.74 (s × 2, 1H × 2), 3.70−3.57 (2H × 2), 3.45 (quartet, 1H × 2, J = 7.1 Hz), 3.42−3.38 (1H × 2), 3.32−3.27 (1H × 2), 2.64 (t, 2H, J = 6.6 Hz), 2.58−2.44 (1H × 2), 2.46 (t, 2H, J = 6.6 Hz), 2.19−2.10 (1H × 2), 1.25 (t, 6H × 2, J = 7.1 Hz), 1.27−1.09 (12H × 2); ^{13}C NMR (100 MHz, $CDCl_3$) δ = 183.5, 158.4, 152.1, 150.6, 146.7, 145.5 (d), 144.8 (d), 139.8 (d), 136.1 (m), 132.2 (d), 131.2, 131.1, 130.1 (d), 128.3 (d), 127.7, 127.5, 126.6 (d), 125.9, 124.8, 121.2, 117.4 (d), 113.1, 109.5, 105.6, 96.2, 86.3 (d), 86.2, 86.0 (d), 80.1 (d), 75.9 (m), 64.1 (d), 58.3 (m), 55.1, 45.0, 43.4 (d), 43.2 (m), 29.6, 24.5 (m), 20.3 (d), 20.1 (d), 12.5; ^{31}P NMR (161.7 MHz, $CDCl_3$, external H_3PO_4 standard) δ = 144.2, 143.9; FABMS, *m*/*z* 937 [(M + H)$^+$]; HRMS calcd for $C_{55}H_{62}N_4O_8P$ [(M + H)$^+$] 937.4305, found 937.4307.

Oligodeoxynucleotide Synthesis and Characterization. Oligodeoxynucleosides (ODNs) were synthesized by a conventional phosphoramidite method using an Applied Biosystems 392 DNA/RNA synthesizer. ODNs were purified by reversed phase HPLC on a 5-ODS-H column (10 mm × 150 mm), eluted with a solvent mixture of 0.1 M triethylammonium acetate (TEAA), pH 7.0, linear gradient over 30 min from 5% to 25% acetonitrile at a flow rate of 3.0 mL/min. The purity and concentration of the synthesized ODNs containing modified nucleotides were determined by complete digestion with calf intestine alkaline phosphatase (50 U/mL), snake venom phosphodiesterase (0.15 U/mL), and P1 nuclease (50 U/mL) to 2′-deoxymononucleosides at 37 °C for 3 h.

Melting Temperature (T_m) Measurement. Melting temperature of the duplex (2.5 μM duplex concentration) was measured with a spectrophotometer equipped with a Peltier temperature controller using a 1-cm path length cell in a buffer containing 50 mM sodium phosphate (pH 7.0) and 100 mM sodium chloride.

Thermodynamics of the Helix-to-coil Transition. The relationship between melting temperatures of heteroduplexes and thermodynamic parameters for the helix-to-coil transition is represented

by the following equation:

$$1/T_m = \Delta S/\Delta H + R\cdot\ln(C_t/4)/\Delta H \quad (1)$$

where C_t is the total strand concentration. In accordance with eq 1, ΔH and ΔS were determined by plotting $(T_m)^{-1}$ versus $\ln(C_t/4)$. We measured the melting temperature of the sample with varying total ODN strand concentrations; 10, 5, 2.5, 1.25 μM.

Fluorescence Measurement. All fluorescence spectra of ODN duplexes (2.5 μM, duplex concentration) were taken in a buffer containing 50 mM sodium phosphate (pH = 7.0) and 100 mM sodium chloride.

The value of the binding constant K_b for the inclusion complex was calculated using the following equation:

$$1/(I - I_0) = 1/(K_b(I_1 - I_0)[CD] + 1/(I_1 - I_0') \quad (2)$$

where [CD] represents the analytical concentration of β-cyclodextrin, I_0 represents the fluorescence intensity of free Nile Red, I_1 is the fluorescence intensity of the inclusion complex, and I is the observed fluorescence intensity at its maximum.

Supporting Information Available: ^{1}H and ^{13}C NMR spectra. This material is available free of charge via the Internet at http://pubs.acs.org.

JO060168O